Phase separation and microstructural characteristics of undercooled Cu-Pb immiscible alloy*

HAN Xiujun (韩秀君)**, WANG Nan (王 楠) and WEI Bingbo (魏炳波)

Laboratory of Materials Science in Space, Department of Applied Physics, Northwestern Polytechnical University, Xi'an 710072, China

Received November 13, 2000; revised December 28, 2000

Abstract Bulk samples of Cu-80% Pb hypermonotectic alloy were undercooled by up to 270 K ($0.21\,T_L$) with glass fluxing technique. The undercooling behavior and the final microstructure were investigated experimentally. It was found that the macrosegregation decreased with the increase of undercooling exponentially. When undercooling reached 270 K, the volume fraction of macrosegregation was reduced by one order of magnitude. Meanwhile, high undercooling brought about significant changes to the microstructural morphology of S(Cu) phase. At small undercoolings, S(Cu) phase grew in dendritic manner. As undercooling increased, S(Cu) dendrite transformed gradually to spherical shell. This morphology transition was ascribed to the concurrent action of the phase separation within miscibility gap and the subsequent solidification process of L_2(Pb) matrix. As an essential step to model the final microstructure, theoretical calculations related to the nucleation of L_1(Cu) droplets were carried out.

Keywords: rapid solidification, high undercooling, phase separation, immiscible alloy.

In the past several decades, the solidification of immiscible alloys has aroused great research interest for two reasons. Firstly, it provides a possible way to produce *in situ* composite materials which can find many applications, such as ductile high-temperature superconductors and self-lubricating bearing alloys[1]. Secondly, the phase separation and crystal growth kinetics during monotectic transformation are of great interest to fundamental research. So far, the unidirectional solidification of monotectic alloys has been well studied and used to prepare fibrous composites[2~4]. Meanwhile, with the development of materials science in space, numerous experiments in outer space have been performed[5~7] to get homogeneous composite materials under microgravity conditions. Unfortunately, some non-gravity-driven effects such as Marangoni convection frequently impedes this possibility and leads to inhomogeneity. In addition to these microgravity experiments, there has been intensive work to search for new casting processing which can help to produce the desired microstructures on ground. The rapid solidification of immiscible alloys seems to be a possible way to realize such a purpose. Up to now, two different routes, i.e. the traditional rapid quenching and high undercooling techniques, have been developed to achieve rapid solidification of alloy melt. The first route has been widely applied to process the immiscible alloys and proved to be effective in many cases[8]. In contrast, there

* Project supported by the National Natural Science Foundation of China (Grant No. 59871040) and Huo Yingdong Education Foundation (Grant No. 71044).

** E-mail address: bbwei@nwpu.edu.cn

have been very few successful investigations on the rapid solidification of undercooled monotectic alloys through the second route. Therefore, much more work is still required to shed further light on the undercooling behavior and rapid solidification kinetics of immiscible alloys.

Cu-Pb monotectic alloy system plays an important role in the research on monotectic solidification and has been extensively studied. The unidirectional solidification investigations show that high growth velocities can yield fibrous composites[4], which is in accordance with Cahn's prediction that composite growth is possible when the directional solidification rate is so high that it can overcome the disjoining pressure which prevents L_2(Pb) and S(Cu) from coming into contact with each other[9]. Under microgravity conditions, macrosegregation still occurs due to some non-gravity-driven effects like Marangoni convection, although the gravity-driven sedimentation of L_2(Pb) is eliminated[6,7].

In our previous work, the undercooling behavior and rapid solidification kinetics of some Cu-Pb monotectic alloys have already been studied[10~12]. It was observed that whether there existed composite structure depended not only on undercooling level but also on alloy composition. Concerning Cu-20% Pb hypomonotectic alloy[10] and Cu-45% Pb hypermonotectic alloy[11], monotectic transformation does not produce any composite structure regardless of the magnitude of undercooling. S(Cu) phase always grows in a dendritic way and exhibits a kinetics feature of solute diffusion controlled growth. However, in the case of Cu-37.4% Pb monotectic alloy[12], a kind of dendrite-shaped monotectic cell came into being as a result of rapid solidification when undercooling exceeded a critical value. In these monotectic cells, both S(Cu) and L_2(Pb) phases grow in a coupled way. As for the influence of undercooling on macrosegregation, there has not been a definite conclusion yet. But to Cu-45% Pb hypermonotectic alloy[11] and Cu-37.4% Pb monotectic alloy[12], large undercooling tends to facilitate phase separation and cause more serious macrosegregation of L_2(Pb) phase.

The objective of the present work is to undercool the bulk samples of Cu-80% Pb hypermonotectic alloy to a significant extent and investigate its microstructural characteristics in a large undercooling range.

1 Experimental procedure

The experiment was performed by glass fluxing method with an apparatus described in Ref. [12]. Cu-80% Pb hypermonotectic alloy samples were prepared by an *in situ* alloying procedure from 99.999% pure Cu and 99.99% pure Pb. A glass with the composition of 70% Na_2SiO_3 + 17.73% $Na_2B_4O_7$ + 12.27% B_2O_3 was used as fluxing agent after having been dehydrated at 1173 K. The sample was superheated to 1373 ~ 1473 K, which is well above the consolute temperature (1263 K) of the miscibility gap to ensure homogenization. Each sample had a mass of 0.6 ~ 1.2 g and was contained in an alumina crucible together with a suitable amount of fluxing agent. The crucible had an inner diameter of 8 mm, an outer diameter of 10 mm and a depth of 12 mm. A NiCr-NiSi thermocouple was used to record the cooling curve and subsequently to determine the undercooling level of the sample. In order to detect the starting point of monotectic solidification more accurately, another NiCr-NiSi thermocouple was applied to form a differential thermocouple with the previous one. Both the crucible and the thermocouples were sealed within a quartz tube with an inner diameter of 15 mm and a length of 250 mm. The quartz tube was evacuated to 5×10^{-2} Pa and then backfilled with Ar gas.

After three times of evacuation-backfilling operation, the experiment was finally accomplished under 90kPa Ar atmosphere. No special cooling means other than removal of the resistance-heating furnace was applied. The average cooling rate was about 20K/s under such a condition. In order to remove as much heterogeneity as possible, the process of heating and cooling was often repeated for 3 ~ 5 times. After experiment, the samples were sectioned, mounted and polished according to standard metallographic procedures. The metallographic specimens were analyzed with an XJG-05 optical microscope for their structural morphologies.

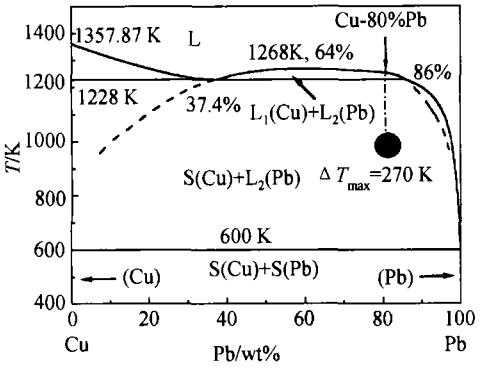

Fig. 1 Designation of composition and undercooling range on Cu-Pb phase diagram[13].

2 Results and discussions

Cu-80% Pb hypermonotectic alloy is located near the right terminal of monotectic horizontal on Cu-Pb phase diagram[13], as shown in Fig. 1. The temperature interval from the binodal line, T_L, to the monotectic horizontal, T_m, is only 35 K. Under equilibrium solidification conditions, both $L_1(Cu)$ and $L_2(Pb)$ liquid phases start to separate from the parent liquid phase, $L \rightarrow L_1(Cu) + L_2(Pb)$, as soon as the temperature falls below 1263 K. The compositions of $L_1(Cu)$ and $L_2(Pb)$ phases change along the binodal line in the miscibility gap. According to the lever rule, a volume fraction of 13.5% is predicted for $L_1(Cu)$ phase at a temperature just above the monotectic horizontal. Immediately after the monotectic transformation $L_1(Cu) \rightarrow S(Cu) + L_2(Pb)$ at 1228 K, the microstructure is composed of 7.9% S(Cu) and 92.1% $L_2(Pb)$. The $L_2(Pb)$ phase diminishes gradually as the temperature drops down and is completely consumed by the eutectic transformation $L_2(Pb) \rightarrow S(Cu) + S(Pb)$ at 600 K. At room temperature, the volume fraction of S(Cu) phase increases to 24.0%.

2.1 Microstructural variation with undercooling

A maximum undercooling of 270 K ($0.21T_L$) has been attained by glass fluxing method, which is far beyond the miscibility gap and has exceeded the critical $0.2T_L$ level for homogeneous nucleation predicted by the classical nucleation theory. A large undercooling represents a state far from thermodynamic equilibrium, and thus the actual solidification mechanism may be different from that of equilibrium.

It was observed that the solidified microstructure depended strongly on undercooling level prior to the monotectic transformation. Fig. 2 presents the low magnification morphologies of Cu-80% Pb hypermonotectic alloy at different undercoolings. Evidently, when undercooling is small, the microstructure is mainly characterized by macrosegregated Cu-rich phase on the upper part of the sample and S(Cu) dendrite embedded in S(Pb) matrix. It is interesting that S(Pb) macrosegregation was also found on the sample top, which is quite similar to the case of Cu-45% Pb alloy[11] and must have been caused by the pushing effect of S(Cu) phase during its floating process.

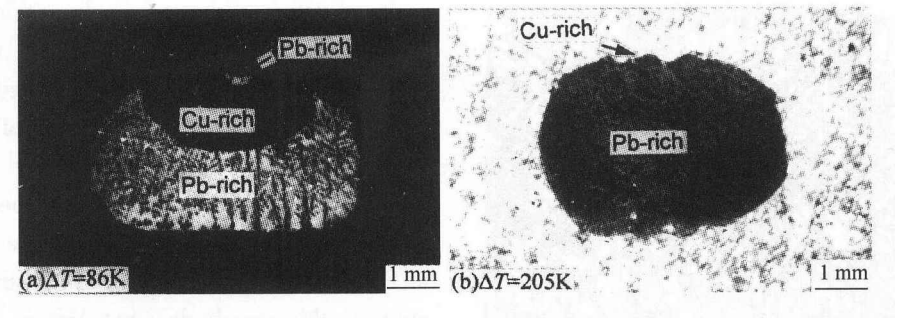

Fig. 2 Macrostructural morphologies of Cu-80% Pb alloy at different undercoolings.

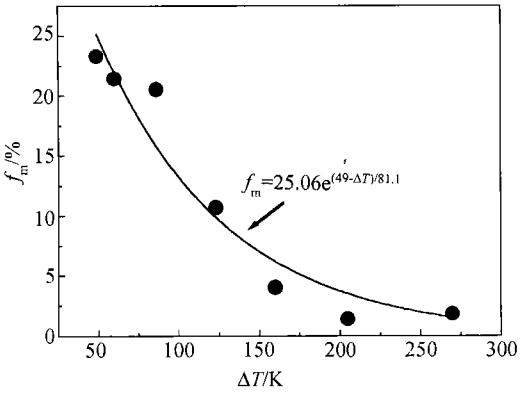

Fig. 3 Volume fraction of macrosegregated Cu-rich phase versus undercooling. ● Experimental data; —— fit.

The increase of undercooling brought about two conspicuous features to the final microstructure. Firstly, the macrosegregation decreased with the increase of undercooling. A remarkable decrease of macrosegregation can be noticed by a comparison between Fig. 2 (a) and Fig. 2 (b). The macrosegregation was nearly eliminated when undercooling attained 205 K. Microstructure analysis shows that the volume fraction of the macrosegregated Cu-rich phase, f_m, is related to ΔT by an exponential law as shown in Fig. 3.

$$f_m = 25.06e^{(49-\Delta T)/81.1}. \quad (1)$$

At the maximum undercooling of 270 K, f_m is reduced to about 1.7%, which is approximately one fourteenth of that in the sample undercooled by 49 K.

Secondly, a great change in structural morphology of S(Cu) phase took place with the enhancement of undercooling. Fig. 4 presents the microstructural variation of Cu-80% Pb hypermonotectic alloy with undercooling, where the white phase is S(Cu) and the black phase S(Pb). Fig. 4 (a) is the magnification of S(Cu) dendrites in Fig. 2 (a). Interestingly, it was noted that several S(Cu) dendrites, as marked by arrows in graph, grew epitaxially from a kind of composite structure composed of outer spherical shell of S(Cu) phase and inner S(Pb) fillings. The above phenomenon indicated that the composite structure formed initially and then the S(Cu) dendrite developed from it. Considering that the composite structure is the product of monotectic transformation, a conclusion can be reached that S(Cu) dendrite is formed during monotectic transformation and grows during subsequent solidification of L_2(Pb) matrix. As undercooling increases, the stem diameter and the secondary arm spacing of S(Cu) dendrite decrease. Once undercooling exceeds a critical value of about 205K, the S(Cu) dendrite feature becomes ambiguous, and its typical morphology evolves into a kind of skeleton, inside which S(Pb) phase distributes, as demonstrated in Fig. 4 (b). The three-dimensional structural model of this composite structure is an interpenetrating and intercrossing network of S(Pb) and S(Cu), which suggests the nature of coupled growth of S(Cu) and L_2(Pb) during monotectic transformation. At further increased undercoolings, the sample is almost totally solidified as spherical com-

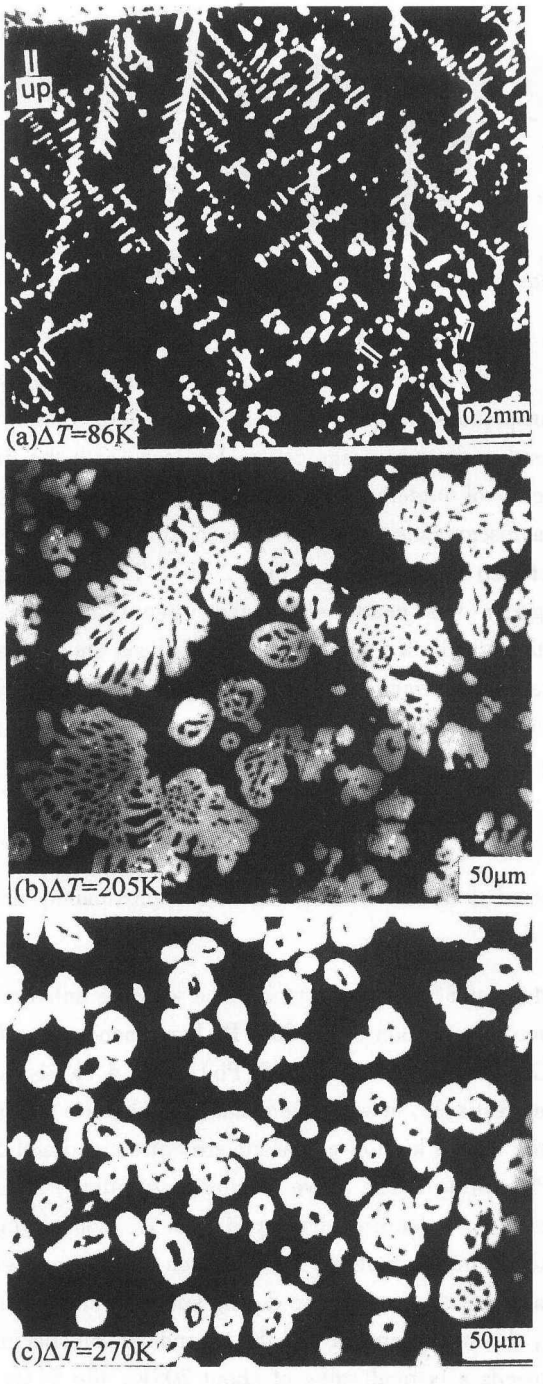

Fig. 4 Solidification microstructures of Cu-80% Pb hyper monotectic alloys at different undercoolings.

posite structure dispersed finely within S(Pb) matrix. Fig. 4 (c) shows the structural morphologies of a sample undercooled by 270 K. The composite structure consists of an outer spherical shell of S(Cu) phase and the surrounded S(Pb) phase. In this aspect, it is much similar to the marked composite structure in Fig. 4 (a). The difference is that the S(Cu) phase in this sample does not develop into dendrite. The size distributions of S(Cu) grains measured from the lower part and the upper part of the sample are illustrated in Figs. 5 (a) and (b), respectively. It is noted that the size spectrum at the lower half part is a truncated Gaussian distribution with a mean value of about 24.6 μm. In contrast, S(Cu) phase on the upper half part shows a wide grain size distribution and the mean value increases to 37.2 μm. Fig. 6 demonstrates the largest radius of S(Cu) grain observable in the examined section versus the normalized distance, defined as the ratio of the position measured from bottom, x, to sample height, h. Obviously, the further from the bottom, the larger is the radius of the largest observable S(Cu) grain. This, in fact, reflects the influence of the gravity-driven sedimentation on the solidified microstructure.

In order to understand such a morphology transition, the phase separation within the miscibility gap and the subsequent solidification process should be considered, because the final microstructure depends strongly on the concurrent action of these two factors[14,15]. The former determines the spatial distribution, the size spectrum and the volume fraction of L_1(Cu) droplets dispersed in L_2(Pb) matrix just before the onset of monotectic transformation. And this will influence the developing interspace and thus the morphology of S(Cu) phase, because each L_1(Cu) droplet dispersed in L_2(Pb) matrix will be developed into one composite structure during monotectic transformation. The latter involves the growth direction of S(Cu) phase and also limits the duration the S(Cu) phase is allowed to grow after

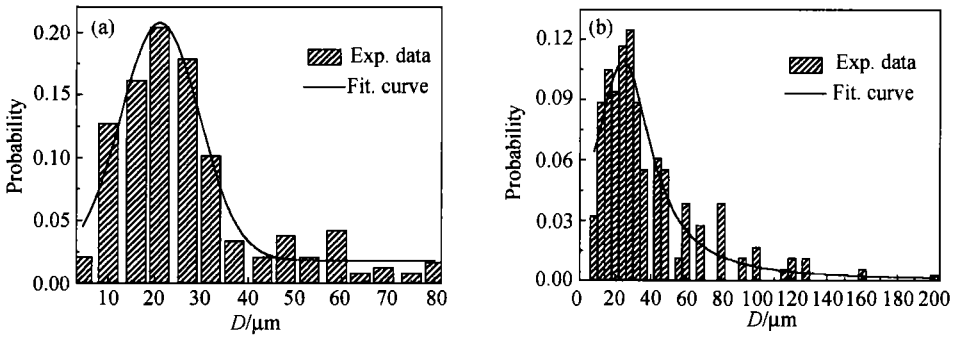

Fig. 5 Size distribution of S(Cu) grains measured in different parts of the sample. (a) The lower part of the sample; (b) the upper part of the sample.

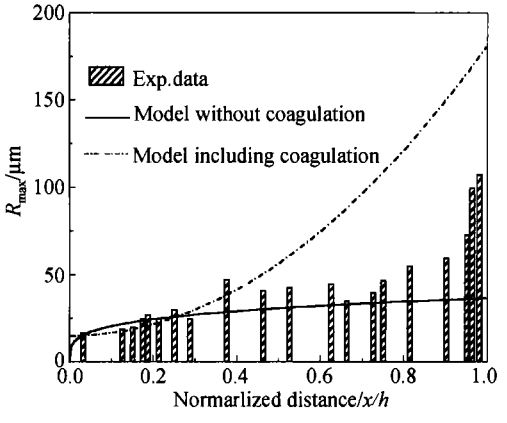

Fig. 6 Measured and calculated largest observable radius of S(Cu) grains as a function of position.

monotectic transformation.

At small undercoolings, when the homogeneous alloy melt is cooled into the miscibility gap, rapid separation of the two liquids will result from the gravity-driven Stokes motion. As a result, only few quite small L_1(Cu) droplets will still be dispersed in L_2(Pb) matrix, because the velocity of Stokes motion is proportional to the square of droplet radius. During the subsequent monotectic solidification process, the latent heat will be absorbed by L_2(Pb) matrix, and thus the interface between L_1(Cu) and L_2(Pb) has the lowest temperature in L_1(Cu) phase and will solidify first. As a result, S(Cu) phase will exist in the form of spherical cell and grow inwardly. Meanwhile, L_2(Pb) phase formed during monotectic transformation will be pushed to the center of L_1(Cu) droplet. Therefore, immediately after monotectic transformation, the composite structure is composed of the outer S(Cu) phase spherical shell and the inside L_2(Pb) phase, just as marked in Fig. 4(a). The small volume fraction of dispersed L_1(Cu) droplet, thus of composite structure after monotectic transformation, makes S(Cu) phase have sufficient interspace to develop. In addition, the rather slow solidification rate endows S(Cu) phase with enough time to grow. These two factors together with the constitutional undercooling in front of the solid/liquid interface result in the dendritic growth of S(Cu) phase.

However, it is not the case for the sample undercooled by up to 270K. The delay of nucleation of L_1(Cu) droplet and the subsequent rapid monotectic solidification make L_1(Cu) droplets have less time to coagulate by collision and float due to gravity. Therefore, the macrosegregation is greatly eliminated and large volume fraction of spherical L_1(Cu) droplets is finely dispersed in L_2(Pb) matrix. The composite structure just after monotectic transformation also exhibits the characteristic that S(Cu) phase grows around L_2(Pb) droplet, which is quite similar to the case of small undercoolings. The difference is that S(Cu) phase has no enough interspace and time to develop into the S(Cu) dendrite and thus keeps its spherical form in the final microstructure. It should be noted that the S(Cu) phase

in composite structure involves both the primary S(Cu) phase precipitated directly from L_1(Cu) droplet and that formed during monotectic transformation, because the composition of L_1(Cu) droplet deviates greatly from monotectic point and is equivalent to that of hypomonotectic alloy under high undercooling conditions, which can be found from the metastable extension of binodal line in the phase diagram. In addition, like Cu-20% Pb hypomonotectic alloy[10], the solid product phase of monotectic transformation must have precipitated onto the existing primary S(Cu) phase. This may be owing to the requirement of the reduction of interfacial energy in quite small droplets.

In the case of the intermediate undercooling range, L_1(Cu) droplets are rather large in volume and exist in irregular form due to the coagulation of L_1(Cu) droplets made by Stokes motion within the miscibility gap. After the formation of S(Cu) spherical shell, the composition of L_1(Cu) reaches monotectic point. Thus, the composite structure shows the typical nature of coupled growth, i.e. S(Cu) phase and L_2(Pb) phase grow alternatively and form an interpenetrating, intercrossing network. Meanwhile, there seems to be a tendency for some S(Cu) grains to develop into dendrites.

2.2 Nucleation of L_1(Cu) droplets

Once the alloy melt is cooled into the two-phase region, L_1(Cu) droplets will nucleate, grow by diffusion, coagulate by collision and float due to gravity. Provided that the solidification process of L_2(Pb) matrix does not change drastically the spatial arrangement of L_1(Cu) droplets, the final microstructure should reflect the interplay of these four processes. The nucleation of L_1(Cu) determines the initial spatial distribution of L_1(Cu) droplets and thus will influence the final microstructure. Therefore, as a first step to model the final microstructure, an understanding of nucleation of L_1(Cu) droplets in parent liquid phase is essential.

The nucleation of droplets in a liquid parent phase can also be described by the classical nucleation theory, as has been proved by Granasy and Ratke[13]. In view that the heterogeneous nucleant has been greatly reduced under high undercooling conditions, the homogeneous nucleation process is assumed in our calculations. Thus, the nucleation behavior of liquid phase can be estimated from the steady state homogeneous nucleation rate[16]:

$$I = \frac{10^{36}}{\eta}\exp\left(-\frac{16\pi\sigma^3}{3k_B T\Delta g^2}\right), \tag{2}$$

where η is viscosity, σ the interface tension between the nucleus and parent phase, Δg the Gibbs free energy difference, and k_B Boltzmann constant.

For liquid-liquid nucleation, the volumetric driving force of decomposition in a binary system, can be given as[14]

$$\Delta g = \left[\Delta G(X) + \left.\frac{\partial G(X)}{\partial x}\right|_{x=X} - \Delta G(X')\right]\cdot \nu_{mol}^{-1}, \tag{3}$$

where ΔG is the Gibbs free energy of mixing, X the initial composition of liquid, X' the composition of the nucleus, while ν_{mol} is the molar volume of the nucleus.

The liquid/liquid interfacial tension is calculated from the following expression[17,18] because of the scarcity of experimental data:

$$\sigma = \frac{6\sqrt{2}\Omega(X' - X)^2}{N_A Z a^2}, \tag{4}$$

where $\Omega = 30261$ (J/mol) is the interaction parameter neglecting the dependence of composition according to CALPHAD[19], N_A the Avogadro constant, $Z = 12$ the number of nearest atoms, and $a = 0.361$ nm the lattice parameter of S(Cu).

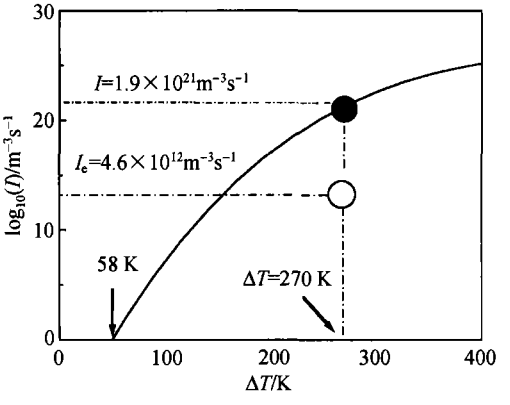

Fig. 7 Homogeneous nucleation rate of L_1(Cu) phase versus undercooling.

During calculation, Timucin's result of the Gibbs free energy of mixing[20] is used, while the other parameters required are taken from Smithell's compilation[21]. Meanwhile, it is assumed that the composition of L_1(Cu) changes along the binodal line and its metastable extension, as shown in Fig. 1. Fig. 7 presents the calculated homogeneous nucleation rate of L_1(Cu) phase versus undercooling. It can be seen that the critical undercooling for homogeneous nucleation rate of L_1(Cu) droplet to exceed 1 m^{-3} s^{-1} is 58 K, and when undercooling attains 270 K the nucleation rate of L_1(Cu) reaches 1.9×10^{21} m^{-3} s^{-1}. Therefore, it is reasonable to say that the homogeneous nucleation of L_1(Cu) is possible.

The nucleation rate of L_1(Cu) droplet at a certain undercooling level can also be estimated from the microstructure analysis in terms of the following expression:

$$I_e = n(\nu t)^{-1}, \tag{5}$$

where n is the total number of S(Cu) grain in the given volume ν, and t the nucleation time.

Assuming a time independent nucleation rate and further assuming that the nucleation event occurs during the whole process that the alloy melt goes through the miscibility gap, the nucleation rate of the sample undercooled by 270 K is estimated as $I_e = 4.6 \times 10^{12}$ $m^{-3}s^{-1}$. Obviously, the calculated result is far larger than the nucleation rate estimated from solidified microstructure. A possible explanation of this deviation is that the number of S(Cu) grains in a given volume will decrease remarkably due to the coalescence and coagulation of L_1(Cu) droplets.

With the estimated nucleation rate I_e, the largest observable radius of L_1(Cu) droplet as a function of position in the sample undercooled by 270 K can be predicted according to the model given by Alkemper and Ratke[15]:

$$r_{max} = x^{9/4} \cdot \Gamma, \tag{6}$$

with

$$\Gamma = \frac{4}{135} I \cdot \sqrt[4]{DS/w_0^5}, \quad S = \frac{c_0 - c_\alpha}{c_\alpha - c_\beta},$$

$$w_0 = \frac{2(\rho - \rho')(\eta - \eta')}{3\eta(2\eta + 3\eta')} g,$$

where I is the estimated nucleation rate from experiment, D diffusion coefficient of Cu atoms in L_2 (Pb) matrix, x the location measured from bottom, c_0 the initial composition, c_α, c_β the Cu concentration at given temperature in the matrix and droplets, η and η' are viscosity of matrix and droplet, while ρ and ρ' are their densities and g the gravity acceleration.

The dashed line in Fig. 6 is the calculated result from Eq. (6). It is shown that up to approximately one third of the sample length the theoretical prediction agrees well with the observed maximum radius, but strong deviations occur to larger particles beyond 0.4 length of the sample. This is caused by the overestimation of the effect of coagulation, because the model considers only the simplest form of coagulation, i.e. any droplet will catch up the whole volume content of the droplet which is just in the cylindrical volume above it.

The solid line in Fig. 6 is drawn on the basis of the expression given by Ratke[15] on condition that the effect of coagulation is neglected.

$$r_{max} = \sqrt[4]{4SDx/w_0}. \tag{7}$$

It seems that the theoretical model without coagulation gives the lower bound of the largest observable radius, while the one that considers the simplest form of coagulation frames presents the upper bound. Evidently, if more details of coagulation are taken into consideration, better agreement between the experimental value and theoretical prediction will be achieved.

3 Conclusions

Bulk samples of Cu-80% Pb hypermonotectic alloy have been undercooled by a maximum of 270 K(0.21 T_L). The microstructures depend strongly on the undercooling level prior to monotectic transformation. At small undercoolings, the microstructure is mainly characterized by serious macrosegregation and S(Cu) dendrite embedded in S(Pb) matrix. With the increase of undercooling, the volume fraction of macrosegregated Cu-rich phase on the upper part of the sample decreases according to an exponential law: $f_m = 25.06 \cdot e^{(49 - \Delta T)/81.11}$. When undercooling reaches 270 K, the volume fraction of macrosegregation is reduced by an order of magnitude. Meanwhile, high undercooling brings about significant morphology transitions to S(Cu) phase. As undercooling increases, S(Cu) dendrite transforms gradually to spherical shell. This morphology transition is the result of the concurrent action of phase separation within the miscibility gap and the subsequent solidification process. Theoretical calculations based on the classical nucleation theory indicate that the homogeneous nucleation of L_1 (Cu) droplets is possible. At the maximum undercooling of 270 K, the nucleation rate of L_1(Cu) is predicted to be 1.9×10^{21} $m^{-3}s^{-1}$, which is much higher than the estimated 4.6×10^{12} $m^{-3}s^{-1}$ from

the final microstructures. This deviation is partially ascribed to the coalescence and coagulation process of L_1(Cu) droplets. With the estimated nucleation rate, the largest observable radius in the solidified microstructure can be predicted according to the model given by Ratke.

Acknowledgements The authors are grateful to Mr. Xie Wenjun, Dr. Zhu Dingyi and Mrs. Lu Xiaoyun for their helpful discussions.

References

1 Predel, B. et al. A European perspective. In: Fluid Sciences and Materials Science in Space, New York: Springer-Verlag, 1987, 517—565.
2 Derby, B. et al. A criterion for the determination of monotectic structure. Acta Metall., 1983, 31: 1123.
3 Kamio, A. et al. Solidification structure of monotectic alloys. Mater. Sci. Eng., 1991, A146: 1005.
4 Grugel, R. N. et al. Alloy solidification in systems containing a liquid miscibility gap. Metall. Trans., 1981, 12A: 669.
5 Carlberg, T. et al. The influence of microgravity on the solidification of Zn-Bi immiscible alloys. Metall. Trans., 1980, 11A: 1665.
6 Shah, S. et al. Directional solidification of lead-copper immiscible alloys in a cyclic gravity environment. Metall. Trans., 1988, 19A: 2677.
7 Sandlin, A. C. et al. The influence of interfacial energies and gravitional levels on the directionally solidified structures in hypermonotectic alloys. Metall. Trans., 1988, 19A: 2665.
8 Chattopadhyay, K. et al. Rapid solidification and decomposition of a hypomonotectic Al-Cd alloy. J. Mater. Sci., 1980, 15: 685.
9 Cahn, J. W., Monotectic composite growth. Metall. Trans., 1979, 10A: 119.
10 Dong, C. et al. Dendritic solidification of undercooled Cu-20% Pb hypomonotectic alloy. Scripta Mater., 1996, 34: 1523.
11 Wei, B. et al. Rapid solidification of undercooled Cu-45% Pb hypermonotectic alloy. Rapidly Quenched and Metastable Materials (Proceedings of RQ9 International Conference, Bratislava, Slovakia, August 25 ~ 30, 1996, ed. by Duhaj, P.), Drichlet: Elsevier Science Publishers, 1997, 14.
12 Dong, C. et al. Monotectic structures of undercooled Cu-37.4% Pb alloy. J. Mater. Sci. Lett., 1996, 15: 970.
13 Massalski, T. B. Binary Alloy Phase Diagrams. ASM, Metal Park, OH, 1986, 946.
14 Granasy, L. et al. Homogeneous nucleation within the liquid miscibility gap of Zn-Pb alloys. Scripta Metall. Mater., 1993, 28: 1329.
15 Alkemper, J. et al. Concurrent nucleation, growth and sedimentation during solidification of Al-Bi alloys. Z. Metallkd., 1994, 85(5): 365.
16 Thompson, C. V. et al. Homogeneous crystal nucleation in binary metallic melts. Acta Metall., 1983, 31: 2021.
17 Dong, C. et al. Solidification kinetics and microstructure evolution of undercooled Fe-Cu melts. Inter. J. Non-Equ. Proc., 1998, 10: 241.
18 Busch, R. et al. Microstructure development during rapid solidification of highly supersaturated Cu-Co alloys. Acta Metall. Mater., 1995, 43: 3467.
19 Chakrabarti, D. J. et al. The Cu-Pb system. Bull. Alloy Phase Diagr., 1984, 5: 503.
20 Timucin, M. Thermodynamic properties of liquid Copper-Lead alloys. Metall. Trans. B, 1980, 11: 503.
21 Brandes, E. A. (ed.). Smithells Metals Reference Book, 6th edition, London: Butterworth & Co. Ltd., 1983.